THE JOURNAL OF BIOLOGICAL CHEMISTRY
Vol. 279, No. 24, Issue of June 11, pp. 24935–24943, 2004
Printed in U.S.A.

Structural and Functional Characterization of the Dimerization Region of Soluble Guanylyl Cyclase*

Received for publication, February 25, 2004
Published, JBC Papers in Press, March 22, 2004, DOI 10.1074/jbc.M402105200

Zongmin Zhou‡, Steffen Gross§, Charis Roussos‡, Sabine Meurer§, Werner Müller-Esterl§, and Andreas Papapetropoulos‡¶‖

From the ‡George P. Livanos-Marianthi Simou Laboratories, Department of Critical Care and Pulmonary Services, Evangelismos Hospital, University of Athens School of Medicine, Athens 10675, Greece, the §Institute for Biochemistry II, University of Frankfurt Medical School, Theodor Stern-Kai 7, Frankfurt D-60590, Germany, and the ¶Laboratory of Molecular Pharmacology, Department of Pharmacy, University of Patras, Patras 26504, Greece

Soluble guanylyl cyclase (sGC) is a ubiquitous enzyme that functions as a receptor for nitric oxide. Despite the obligate heterodimeric nature of sGC, the sequence segments mediating subunit association have remained elusive. Our initial screening for relevant interaction site(s) in the most common sGC isoenzyme, $\alpha_1\beta_1$, identified two regions in each subunit, *i.e.* the regulatory domains and the central regions, contributing to heterodimer formation. To map the relevant segments in the β_1 subunit precisely, we constructed multiple N- and C-terminal deletion variants and cotransfected them with full-length α_1 in COS cells. Immunoprecipitation revealed that a sequence segment spanning positions 204–408 mediates binding of β_1 to α_1. The same region of β_1[204–408] was found to promote β_1/β_1 homodimerization. Fusion of β_1[204–408] to enhanced green fluorescent protein conferred binding activity to the recipient protein. Coexpression of β_1[204–408] with α_1 or β_1 targeted the sGC subunits for proteasomal degradation, suggesting that β_1[204–408] forms structurally deficient complexes with α_1 and β_1. Analysis of deletion constructs lacking portions of the β_1 dimerization region identified two distinct segments contributing to α_1 binding, *i.e.* an N-terminal site covering positions 204–244 and a C-terminal site at 379–408. Both sites are crucial for sGC function because deletion of either site rendered sGC dimerization-deficient and thus functionally inactive. We conclude that the dimerization region of β_1 extends over 205 residues of its regulatory and central domains and that two discontinuous sites of 41 and 30 residues, respectively, facilitate binding of β_1 to the α_1 subunit of sGC.

The second messenger cGMP plays a critical role in the regulation of smooth muscle tone, platelet aggregation, retinal phototransduction, and neurotransmission (1, 2). It is produced from GTP in a reaction catalyzed by guanylyl cyclase, of which two types exist. The first guanylyl cyclase type includes a family of membrane-bound isoenzymes that are receptors for natriuretic factors and intestinal peptides, and therefore has been dubbed particulate GC (pGC)[1] (3). The second type of guanylyl cyclase was originally thought to be entirely cytosolic and was therefore named soluble guanylyl cyclase (sGC) (4, 5). Indeed, the vast majority of sGC is found in the cytosolic fraction of vascular smooth muscle cells; however, recent evidence suggests that sGC may also associate with synaptosomal membranes of neurons as well as with plasma membranes of endothelial cells and platelets (6–8). Regardless of its subcellular localization, sGC functions as a receptor for nitric oxide (NO), *i.e.* the major endogenous activator of sGC which induces an activity increase of 200–500-fold (5, 9). Carbon monoxide can also stimulate sGC activity though to a lesser extent, up to 5-fold (5, 10). The best studied exogenous sGC activators are organic nitrates, which mimic the action of endogenous NO, *e.g.* in the treatment of angina pectoris. Other activators of sGC have been reported to work independently of NO (YC-1) or heme (BAY 58-2667) (11–13).

Originally sGC was purified as a heterodimeric protein from bovine lung (14). Early evidence indicated that both the large (α) and the small (β) subunits are essential for enzymatic activity because transient expression of either α or β cDNA alone failed to produce NO-inducible cGMP accumulation, whereas cotransfection of both subunits yielded a NO-sensitive enzyme (15, 16). Inhibition of either α or β gene expression using antisense oligonucleotides significantly attenuated sGC activity (15). Thus heterodimerization appears to be an absolute requirement for the expression of sGC activity. To date, two isoforms for each sGC subunit have been identified, *i.e.* α_1 and α_2 as well as β_1 and β_2 (17–19). The most common sGC isoform $\alpha_1\beta_1$ is ubiquitously present in the human body, with the nervous system, lung, and liver exhibiting the highest levels of expression (20). The $\alpha_2\beta_1$ dimer is most abundant in brain, uterus, and placenta (20, 21). The mRNA for human β_2 is expressed in kidney and liver (19); however, the corresponding dimers such as $\alpha_1\beta_2$ or $\alpha_2\beta_2$ have not been identified *in vivo*. Recently, α_1/α_1 and β_1/β_1 homodimers lacking cyclase activity were reported to coexist with $\alpha_1\beta_1$ in transfected cells overexpressing both sGC subunits (22).

To date the three-dimensional structure of sGC is still unknown. Based on structural comparisons with pGC and adenylyl cyclases, each sGC subunit has been divided arbitrarily into

* This work was supported by Greek Secretariat of Research and Technology Grant PENED 2001/01EΔ67, University of Athens Grant 70/4/5918, and the Thorax Foundation (to A. P.) and by the Deutsche Forschungsgemeinschaft and the Fonds der Chemischen Industrie (to W. M.-E.). The costs of publication of this article were defrayed in part by the payment of page charges. This article must therefore be hereby marked "*advertisement*" in accordance with 18 U.S.C. Section 1734 solely to indicate this fact.

‖ To whom correspondence should be addressed: George P. Livanos Laboratory, University of Athens, School of Medicine, Ploutarchou 3, 5th floor, Athens 10675, Greece. Tel.: 30-210-721-7467; Fax: 30-210-721-9417; E-mail: apapapet@upatras.gr.

[1] The abbreviations used are: pGC, particulate guanylyl cyclase; CBS, C-terminal binding site; EGFP, enhanced green fluorescent protein; GST, glutathione *S*-transferase; NBS, N-terminal binding site; NO, nitric oxide; sGC, soluble guanylyl cyclase; VSV, vesicular stomatitis virus.

three major domains: an N-terminal region containing the regulatory domain, a central region, and a C-terminal region comprising the catalytic domain (23, 24). The catalytic domains of α_1 and β_1 consist of ~250 residues, and they are the best conserved regions between the various subunits and among sGCs from various species. The regulatory domain of β_1 contains a heme binding region where His^{105} links to Fe^{2+} of the prosthetic group (25). The corresponding domain of α_1 does not participate in heme binding but carries a regulatory site at positions 259–364 which is necessary for the activation by NO (26). The central region of the sGC subunits is often referred to as the putative "dimerization domain" based on circumstantial evidence and extrapolation of information available from the sequence mediating homodimerization of pGC (27). *In silico* analyses have predicted that sGC dimerization site(s) are exposed by sequence segments spanning positions 312–377 (28) or 340–384 (29); however, experimental data confirming or refuting these predictions are still lacking.

Here we have set out to map the sequence segments mediating heterodimerization of mammalian sGC subunits. Our main findings are that the dimerization region of the β_1 subunit contacting the α_1 subunit extends over more than 200 residues (positions 204–408), covering the C-terminal half of the regulatory domain and the entire central region. Within this dimerization region we have identified two separate sites, an N-terminal binding site spanning residues 204–244 and a C-terminal binding site at 379–408, each contributing to heterodimerization and thus functional expression of mammalian sGCs.

EXPERIMENTAL PROCEDURES

Materials—Dulbecco's modified Eagle's medium and fetal calf serum were obtained from Invitrogen. Cell culture plasticware was from Greiner (Frickenhausen, Germany). The BL21-codon plus strain of *Escherichia coli* was from Stratagene (La Jolla, CA). Monoclonal anti-V5 antibody, platinum *Pfx* DNA polymerase, and the pcDNA3.1 Directional TOPO Expression kit were from Invitrogen. The cGMP enzyme immunoassay kits were from R&D Systems (Minneapolis). SuperSignal West Pico chemiluminescent substrate was from Pierce. The *DC* protein assay kit, Tween 20, and other immunoblotting reagents were from Bio-Rad. jetPEI transfection reagent was from Polyplus-transfection (Illkirch, France). Protein G-agarose beads and nitrocellulose membrane Hybond ECL were from Amersham Biosciences. All other reagents including agarose beads coupled to glutathione, antibodies to β_1 and VSV (P5D4), penicillin, streptomycin, isobutylmethylxanthine, sodium nitroprusside, bovine serum albumin, phenylmethylsulfonyl fluoride, aprotinin, EGTA, EDTA, and pepstatin were from Sigma.

Antibodies to sGC Subunits—The sequence corresponding to amino acids 1–470 of the α_1 subunit was amplified by PCR and subcloned into the pGEX-Kg vector. The fusion protein of glutathione *S*-transferase and α_1 (GST-α_1) was isolated from BL21-codon plus *E. coli* by standard techniques and used to immunize rabbits. The resulting antibody specifically recognized the α_1 subunit, *i.e.* it did not cross-react with the β_1 sGC subunit. For affinity purification GST-α_1 was cross-linked to glutathione-Sepharose. Alternatively subunit-specific antibodies were raised in rabbits against synthetic peptides derived from human α_1 (residues 94–121) or β_1 (residues 593–614). For affinity purification of the antibodies, the respective peptides were covalently coupled to Affi-Gel 10 (Bio-Rad).

Yeast Interaction Trap Assay—Vectors pEG202 and pJG4-5 and yeast strains EGY48 and RFY206 for the interaction trap assay were generously provided by Roger Brent (Boston). Plasmids expressing human β_1[1–348], β_1[349–403], or β_1[404–619] fused to the LexA DNA binding domain were introduced in yeast strain EGY48 (MATα *trp1 his3 ura3 leu2*::6LexAop-*LEU2*) containing the reporter plasmid pSH18-34. Plasmids expressing β_1[1–348], β_1[349–403], or β_1[404–619] fused to the B42 activation domain were introduced in RFY206 (MATa *trp1::hisG his3Δ200 ura3–52 lys2Δ201 leu2–3*). For mating, cell suspensions of both strains (50 μl each) were mixed and incubated in rich medium (YPD) at 30 °C for 14–16 h. Interactions were validated by growth and blue coloring on minimal agar plates lacking uracil, histidine, tryptophan, and leucine, supplemented with 2% galactose, 1% raffinose, and 80 μg/ml 5-bromo-4-chloro-3-indolyl-β-D-galactopyranoside (X-gal).

Construction of Expression Plasmids for sGC Subunit Mutants—The cDNAs for human sGC α_1 and β_1 fused to an N-terminal VSV epitope were subcloned into a modified pSG5 vector, pSG8VSV(EcX). The cDNAs for rat α_1 with an N-terminal myc-tag, rat β_1 with a C-terminal V5 tag, and deletion mutants thereof were generated by PCR and cloned into the pcDNA3.1/V5-His TOPO vector using standard methodology. All cDNA constructs used in this study were sequenced prior to use.

Transfection of COS Cells—African green monkey kidney COSm6 cells were cultured in Dulbecco's modified Eagle's medium supplemented with 10% fetal calf serum. Cells plated in 6-well plates at a density of 2×10^5 cells/well were grown overnight. Cells were transfected with appropriate plasmids using jetPEI transfection reagent according to the manufacturer's instructions, applying a total of 3 μg of DNA and 6 μl of jetPEI/well. For cotransfection experiments, equal amounts of DNA were used for each plasmid. Alternatively, we used transient transfections of COS1 cells applying the DEAE-dextran method. For a 10-cm dish 5.4×10^5 cells were washed with phosphate-buffered saline, and expression plasmids were applied in 5.7 ml of serum-free medium mixed with 300 μl of DEAE-dextran (1 mg/ml) and 12 μl of chloroquine (50 mg/ml). After incubation for 2.5 h, cells were treated with 10% dimethyl sulfoxide in phosphate-buffered saline for 2 min and cultured in Dulbecco's modified Eagle's medium and 10% fetal calf serum for 30–48 h prior to use.

Immunoprecipitation and Western Blotting—Cells were harvested 30–48 h after transfection and lysed in a buffer containing 1% Triton X-100, 50 mM Tris-HCl, pH 7.5, 150 mM NaCl, 50 mM NaF, 1 mM EDTA, 0.1 mM EGTA, 1 mM Na_3VO_4, 0.5% deoxycholic acid, 0.1% SDS, 10 μg/ml aprotinin, 10 μg/ml pepstatin, and 20 mM phenylmethylsulfonyl fluoride. Cellular debris was pelleted at 12,000 $\times$ *g* for 10 min, the supernatants were collected, and their protein concentrations determined. Cell lysates containing 200–250 μg of protein were incubated overnight at 4 °C with anti-myc or anti-VSV followed by protein G-coupled agarose beads; alternatively, anti-myc conjugated to agarose beads was used. Using 250 μg of total lysate protein and anti-myc for immunoprecipitation, 25–40% of myc-tagged α_1 was recovered from total sGC input. Immunoprecipitated proteins or cell lysates were subjected to SDS-PAGE on 10% polyacrylamide gels and transferred to nitrocellulose membranes. The membranes were blocked with 5% dry milk in TBS-T (10 mM Tris, pH 7.5, 100 mM NaCl, 0.1% Tween 20) for 1 h at room temperature, rinsed, and incubated overnight at 4 °C with primary antibody in 3% milk, TBS-T. Subsequently, the blots were incubated with secondary antibody for 2 h at room temperature. Immunoreactive proteins were detected using the SuperSignal chemiluminescence kit.

cGMP Enzyme Immunoassay—48 h after transfection the cells were washed with Earle's balanced salt solution and incubated in it in the presence of 1 mM phosphodiesterase inhibitor isobutylmethylxanthine for 15 min with or without 100 μM sodium nitroprusside. Media were aspirated, and 0.1 N HCl was added to extract cGMP. After 30 min, HCl extracts were collected, and cGMP was quantified.

Quantitative Reverse Transcription-PCR—Cells (2.4×10^5) were harvested into 500 μl of TriZol (Molecular Research, Cincinnati, OH). Total RNA was extracted and quantified, and 200 ng of each sample was reversely transcribed into cDNA (iSCRIPT cDNA kit, Bio-Rad). Two μl of each cDNA sample was used as template for the amplification reaction carried out with Assays-on-Demand™ Gene Expression Products (Applied Biosystems, Foster City, CA) following the manufacturer's instructions. PCR amplifications were carried out in a Light Cycler System (Bio-Rad) and analyzed with the LightCycler™ IQ software 3.0. The level of target mRNA (sGCα_1) was quantitated by determining the amplification cycle where the respective PCR products were first detected (C_T) and normalized to the endogenous 18 S rRNA level.

RESULTS

Identification of the Segments Involved in α_1/β_1 Heterodimerization—To map grossly the sequence segments involved in sGC dimerization, we dissected the human α_1 and β_1 subunits into three major segments, *i.e.* the N-terminal portion including the regulatory domain (positions 1–419 in α_1 and 1–348 in β_1, respectively), the central region (422–466 and 349–403), and the C-terminal portion comprising the catalytic domain (466–690 and 404–619). Using the yeast interaction trap assay we found that the N-terminal regulatory domains and the central regions of α_1 and β_1 consistently showed mu-

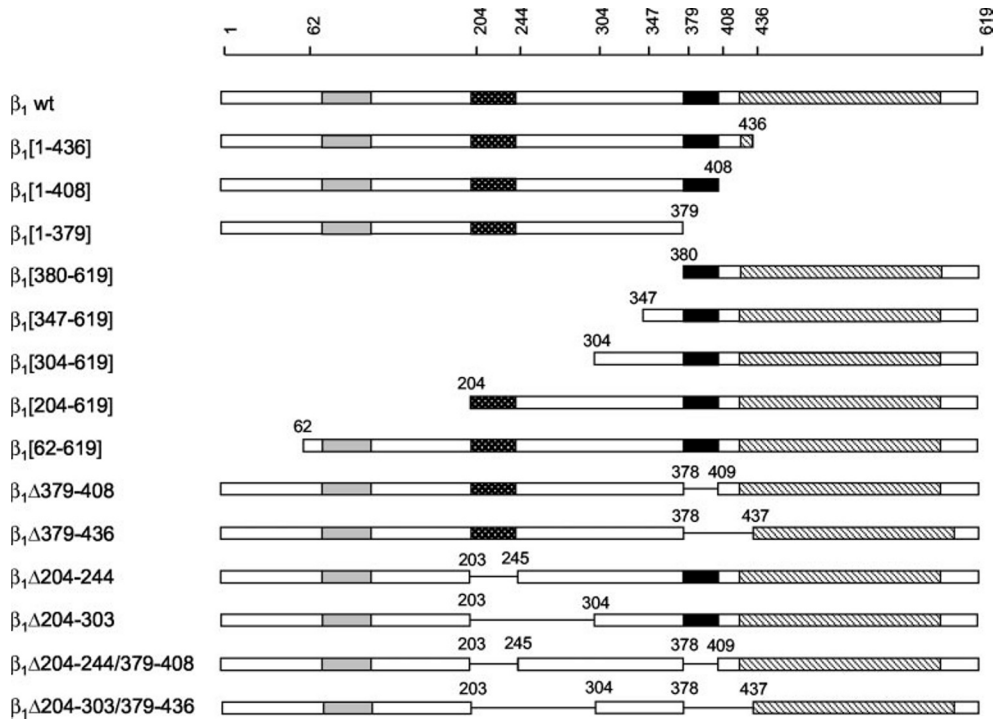

FIG. 1. **Schematic representation of rat β_1 constructs.** The heme binding region is shown in *gray* (residues 80–139), and the cyclase catalytic domain is defined by the *hatched* area (residues 412–606). The NBS (204–244) is represented by the *dotted* area, and the CBS (379–408) is shown in *black*. *Numbers* identify the relative positions in the amino acid sequence. Retained sequences are *bracketed*, and deleted sequences are indicated by the prefix Δ.

tual interactions, whereas other combinations did not (data not shown). In COS cells binding of full-length α_1 to β_1 was sensitive to the deletion of the β_1 central region (positions 349–403) but not of the β_1 catalytic domain (404–619) (data not shown). These initial results pointed to a role of both the N-terminal portions and central regions of the sGC subunits in heterodimer formation.

Studies with N- and C-terminal Truncation Variants of the β_1 Subunit—To define more precisely the sequence segments participating in sGC dimerization, we dissected the rat β_1 subunit which is almost identical to its human homolog (98.5% sequence identity). We generated a number of N-terminal, C-terminal, and internal deletion mutants (summarized in Fig. 1) and coexpressed them with the myc-tagged rat α_1 in COS cells. We first analyzed the deletion mutants where we had progressively shortened the C-terminal portion of β_1 by 183 residues (β_1[1–436]), 211 residues (β_1[1–408]), and 240 residues (β_1[1–379]). Although similar expression levels were achieved for the various forms, only the longer variants β_1[1–436] and β_1[1–408] but not the shortest variant β_1[1–379] lacking the entire catalytic domain and part of the central region were present in anti-myc immunoprecipitates (Fig. 2*A*). In the reverse approach using cells cotransfected with wild-type α_1 and His_6-tagged full-length β_1 or its C-terminal deletion mutants, we coprecipitated α_1 from cell lysates containing full-length β_1 or β_1[1–408] but not from cells expressing β_1[1–379] (not shown). Thus, the C-terminal 211 residues (positions 409–619) of β_1 are dispensable for heterodimerization, whereas residues 380–408 appear to be critical for binding to α_1.

Next we tested V5-tagged β_1 mutants with progressive deletions of the N-terminal portion by 61 (β_1[62–619]), 203 (β_1[204–619]), 303 (β_1[304–619]), 346 (β_1[347–619]), or 379 residues (β_1[380–619]). After coexpression of the β_1 deletion constructs with full-length myc-tagged α_1 followed by immunoprecipitation with anti-myc and Western blotting with anti-V5, we observed that β_1 constructs lacking the first 61 or 203 amino acids fully retain their ability to bind to α_1 (Fig. 2*B*). Further shortening of the N terminus by 303, 346, or 379 residues drastically reduced the presence of β_1 in anti-myc immunoprecipitates, suggesting that the segment spanning positions 204–303 (or parts thereof) may be involved in α_1/β_1 heterodimerization. Importantly, the difference in binding of the β_1 deletion mutants to α_1 cannot be attributed to differences in the expression levels of α_1 or β_1 constructs, nor is it because of different amounts of immunoprecipitated α_1 (*cf.* control panels in Fig. 2*B*). It should, however, be noted that after prolonged exposure faint signals were observed for the β_1[304–619] and β_1[347–619] deletion mutants (not shown). The above data taken together suggest that the sequence segment spanning residues 204–408 of β_1 contains the structural elements mediating heterodimerization with α_1 and that two distinct subsegments extending over positions 204–303 and 380–408 are critically involved in this binding.

Identification of Two Distinct Binding Sites Mediating Heterodimerization—To study further the relative contributions of the various sequence segments for heterodimerization we generated internal deletion mutants of β_1 affecting the critical region between positions 204–408 and coexpressed them with myc-tagged α_1. Binding to α_1 was reduced moderately for full-length β_1 lacking positions 204–244 ($\beta_1\Delta$204–244) or positions 204–303 ($\beta_1\Delta$204–303) and was reduced drastically for deletion mutants $\beta_1\Delta$379–408 and $\beta_1\Delta$379–436 (Fig. 3). Because we did not observe a significant difference in the binding to α_1 between $\beta_1\Delta$204–244 and $\beta_1\Delta$204–303, we concluded that the region spanning residues 245–303 does not contain critical residues for heterodimer formation. Moreover, deletion of the segment 379–408 further reduced the binding affinity of $\beta_1\Delta$204–244 mutant, almost to background level (Fig. 3). Thus it appears that segment 204–408 mediates β_1 binding to α_1 and that the C-terminal portion covering positions 379–408 of β_1 exposes a major binding site for α_1, whereas the N-terminal portion of 204–244 of β_1 contributes a minor interaction site.

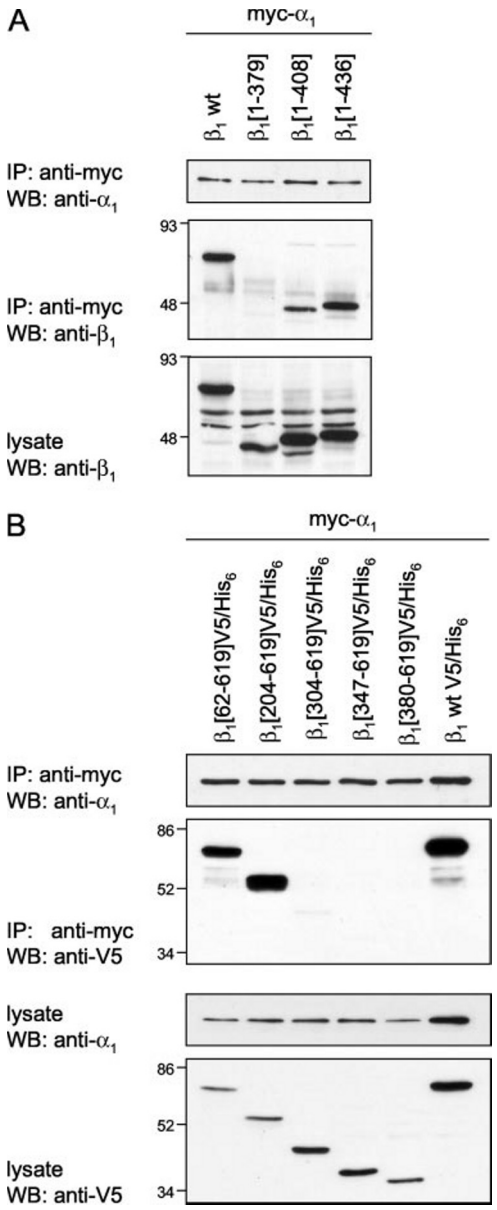

FIG. 2. **Heterodimerization of truncation mutants of β_1.** *A*, COS cells were cotransfected with the cDNAs encoding myc-tagged α_1 and full-length or various deletion mutants of β_1 of rat sGC. Immunoprecipitation (*IP*) was done with anti-myc, and the resultant precipitates were analyzed by SDS-PAGE and Western blotting (*WB*) with an antibody to α_1 (*top*) or β_1 (*middle*). Expression of β_1 deletion mutants was monitored in lysates using anti-β_1 (*bottom*). *wt*, wild-type. *B*, COS cells were cotransfected with cDNAs encoding myc-tagged α_1 and V5-tagged wild-type β_1 or deletion mutants thereof, as indicated. The presence of equal amounts of α_1 in the immunoprecipitates was followed by Western blotting with anti-α_1 (*top*). Immunoprecipitates with anti-myc were analyzed by Western blotting using anti-V5 (*upper middle*). To follow expression levels, cell lysates were blotted with anti-α_1 or anti-V5 (*lower middle* and *bottom,* respectively). Representatives of experiments repeated at least twice with identical results are shown.

Effects of the Expressed Binding Site Segment—If our notion is correct that sequence segment of 204–408 of the β_1 subunit is necessary and sufficient to mediate binding to α_1, we reasoned that (i) full-length α_1 should bind to the critical sequence segment of β_1[204–408] thereby producing an inactive cyclase and that (ii) fusion of β_1[204–408] to an unrelated partner, *e.g.* EGFP, should confer α_1 binding activity to the recipient protein. To test the former assumption, we coexpressed wild-type α_1 with VSV-tagged β_1[204–408] in COS cells and applied an antiserum to α_1 under the same conditions successfully used

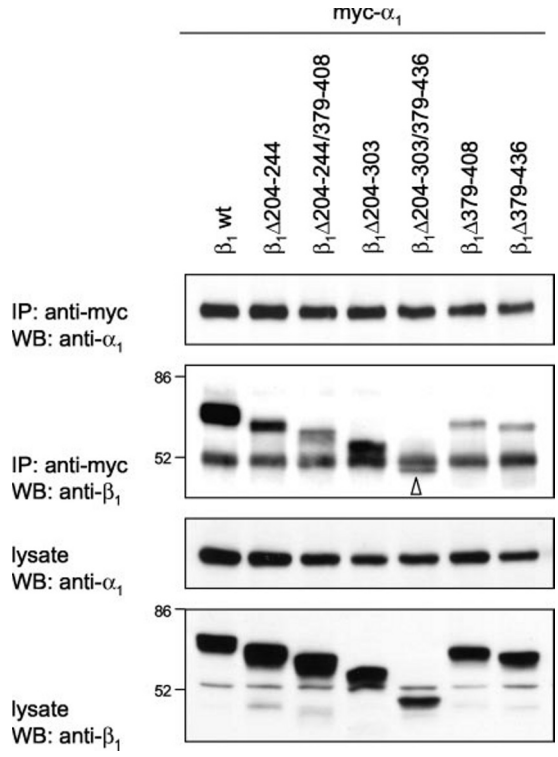

FIG. 3. **Selective deletion of segments from the dimerization region.** COS cells were cotransfected with cDNAs encoding myc-tagged α_1 and wild-type (*wt*) β_1 or its deletion mutants. The presence of equal amounts of α_1 in the immunoprecipitates (*IP*) done with anti-myc was followed by Western blotting (*WB*) using anti-α_1 (*top*). Western blots of the immunoprecipitates were analyzed by anti-β_1 (*upper middle*). To monitor expression levels lysates were blotted with anti-α_1 or anti-β_1 (*lower middle* and *bottom,* respectively). Blots are representative of experiments repeated at least two times with identical results. The *arrowhead* marks the $\beta_1\Delta$204–303/379–436 protein. The designation of the constructs is according to Fig. 1.

for coimmunoprecipitation of the various β_1 mutants (see above). Surprisingly cells cotransfected with β_1[204–408] had greatly reduced α_1 levels compared with cells coexpressing unrelated protein AGAP1-PH (Fig. 4A), and antibodies to α_1 failed to coprecipitate significant amounts of β_1[204–408] (not shown) although the protein was clearly present in cell lysates (Fig. 4*A*). Using real time PCR we found that the relative expression levels of α_1 mRNA were almost identical in the presence of β_1[204–408] or control protein, indicating that α_1 protein was selectively down-regulated in the presence of β_1[204–408]. Indeed coexpresssion of α_1 and increasing amounts of β_1[204–408] revealed a gradual decrease in α_1 protein levels, whereas increasing expression levels of the control protein IA2βcyt did not affect α_1 protein levels (Fig. 4*B*). Thus we reasoned that coexpression of and complex formation with β_1[204–408] targets α_1 for intracellular degradation.

To test this intriguing possibility we incubated cells expressing wild-type α_1 and β_1[204–408] for 12 h in the presence of broad specific proteasome inhibitors MG132 and epoxomycin. Both inhibitors significantly increased the intracellular α_1 protein levels, although they did not fully reverse the effect of β_1[204–408] coexpression (Fig. 4*C*), supporting the idea that β_1[204–408] binding targets wild-type α_1 for proteasomal degradation. To test whether β_1[204–408] may also interfere with the complex formation between the full-length sGC subunits we cotransfected COS1 cells with wild-type α_1 and β_1 and increasing amounts of β_1[204–408]; for control unrelated protein IA2βcyt was used. Increasing levels of β_1[204–408] were paralleled by decreasing levels of α_1 and β_1, and this effect was partially reversed in the presence of the proteasome inhibitor

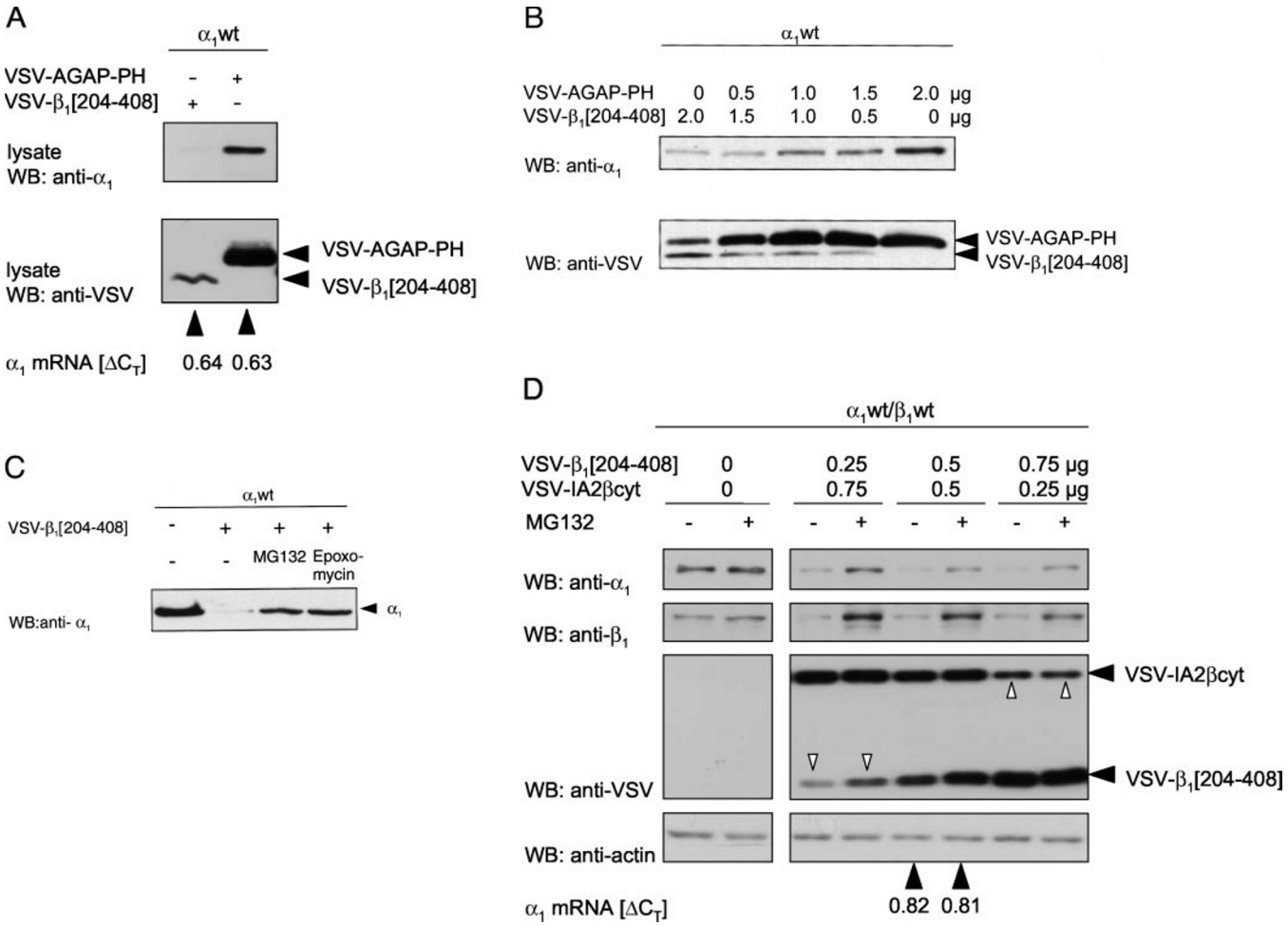

FIG. 4. **Effect of coexpression of β_1 dimerization region on α_1 protein level.** *A*, lysates of COS cells cotransfected with cDNAs encoding α_1 and VSV-tagged β_1[204–408] or unrelated protein AGAP1-PH was analyzed by anti-α_1 (*top*) or anti-VSV (*bottom*). The relative expression levels of α_1 mRNA were quantified by real time PCR at 48 h post-transfection and normalized for endogenous 18 S rRNA (ΔC_T; *arrowheads*). *wt*, wild-type; *WB*, Western blot. *B*, COS cells were cotransfected with 0.5 μg of α_1, decreasing amounts of cDNA encoding VSV-tagged β_1[204–408] (2.0–0 μg), and increasing amounts (0–2.0 μg) of control protein AGAP1-PH. Protein levels were monitored by Western blotting of total cell lysates using anti-α_1 (*top*) or anti-VSV (*bottom*). *C*, COS cells expressing wild-type α_1 in the absence (−) or presence (+) of VSV-tagged β_1[204–408] were incubated for 12 h with (+) or without (−) proteasome inhibitors 10 μM MG132 or 5 μM epoxomycin, as indicated. Protein levels were monitored by Western blotting of lysates using anti-α_1. *D*, COS cells expressing α_1 and β_1 were cotransfected with increasing amounts (0–0.75 μg) of cDNA encoding VSV-tagged β_1[204–408] and control protein VSV-IA2βcyt, as indicated. Cells were preincubated for 12 h in the absence (−) or presence (+) of 10 μM MG132. Western blotting of lysates was done with anti-α_1 (*top*), anti-β_1 (*upper middle*), or anti-VSV (*lower middle*). To monitor protein loading, lysates were probed for actin (*bottom*). The expression levels of α_1 mRNA were quantified by real time PCR and normalized for endogenous 18 S rRNA at 48 h post-transfection (ΔC_T; *arrowheads*). Blots are representative of experiments done at least twice with identical results.

MG132 (Fig. 4*D*, *upper panels*). Under the conditions of this experiment the levels of β_1[204–408] but not those of the control protein were also up-regulated in the presence of MG132 (Fig. 4*D*, *open arrowheads*). Because the α_1 mRNA levels were unchanged (Fig. 4*D*, *bottom*, *arrowheads*) we conclude that coexpression of α_1 and β_1[204–408] results in a dramatic down-regulation of α_1 even at low levels of β_1[204–408], possibly by binding to and targeting of the α_1 subunit for intracellular degradation.

Segment β_1[204–408] Confers Binding Activity to EGFP—To test whether we can confer the α_1 binding capacity to a recipient protein, we fused the relevant sequence segment of β_1 to EGFP. Immunoprecipitation of myc-tagged α_1 coexpressed with EGFP-β_1[200–408] in COS cells demonstrated that anti-myc brought down significant amounts of the EGFP fused to β_1[200–408], whereas the authentic EGFP protein failed to coprecipitate with α_1 protein. By contrast fusion proteins containing a single individual binding site, *i.e.* EGFP-β_1[200–244] for the N-terminal site (not shown) and EGFP-β_1[379–408] for the C-terminal site, failed to coprecipitate with myc-tagged α_1 (Fig. 5). Of note the expression level of α_1 is lowered (but not nullified) in the presence of the β_1 segment spanning the entire binding region (β_1[200–408]), whereas constructs holding full-length β_1 or β_1[379–408] did not change α_1 protein levels compared with unfused EGFP. Thus the region 204–408 of β_1 appears to be necessary and sufficient to mediate heterodimerization with α_1, whereas the individual N- and C-terminal binding sites are necessary but not sufficient to drive the interaction between EGFP and the α_1 subunit.

Functional Significance of the Binding Segment—To test whether the cGMP forming capacity of sGC is affected by the β_1 sites involved in subunit heterodimerization, we initially transfected COS cells overexpressing wild-type α_1 β_1 with increasing levels of β_1[204–408]. Stimulation of cells with sodium nitroprusside resulted in a >30-fold increase in their intracellular cGMP concentration; however, cells that had been cotransfected with β_1[204–408] failed to produce significant amounts of cGMP, even at the lowest expression levels of β_1[204–408]. Likewise, deletion mutant $\beta_1\Delta$204–303, retaining its α_1 binding capacity though at a reduced level, failed to produce cyclase activity when coexpressed with α_1 (not shown). Hence it is likely that the combined effects of functional deficiency result-

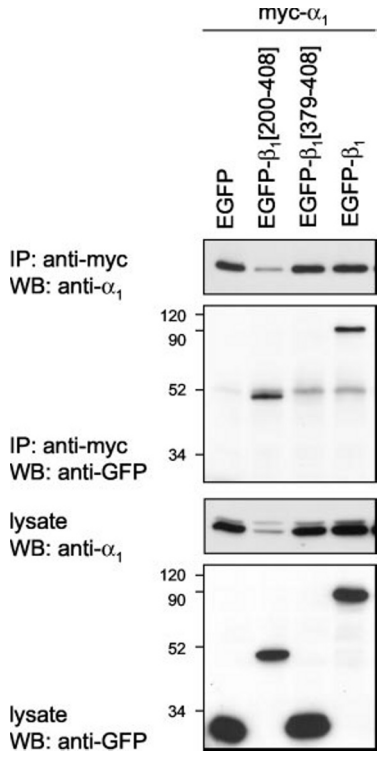

FIG. 5. **Coprecipitation of β_1 dimerization region fused to EGFP.** COS cells were cotransfected with the cDNAs encoding myc-tagged α_1 and EGFP fused to β_1 segments 200–408 or 379–408 or to wild-type β_1. Western blots (*WB*) of the immunoprecipitates (*IP*) using anti-myc were analyzed by anti-α_1 (*top*) or anti-GFP (*upper middle*). To monitor expression levels, lysates were blotted with antibodies to α_1 or to GFP (*lower middle* and *bottom*, respectively). Blots are representative of experiments repeated at least twice with identical results.

ing from failing complementation of the active site as well as proteasomal targeting of sGC subunits abrogated cyclase activity. To overcome this problem we tested EGFP-β_1[204–408] fusion constructs, which reduce α_1 levels without nullifying them (*cf.* Fig. 5). Coexpression of wild-type $\alpha_1\beta_1$ and EGFP-β_1[204–408] showed a moderate though significant inhibition of both the basal and sodium nitroprusside-stimulated cGMP accumulation by 35.2 ± 4.0% and 17.5 ± 3.3%, respectively, indicating that EGFP-β_1[204–408] interferes with sGC activity, possibly by replacing the full-length β_1 subunit in the native $\alpha_1\beta_1$ complex.

Sites Involved in β_1 Homodimerization—Because homodimerization of single subunits has been implicated in limiting the cGMP-generating capacity of cells we asked whether the same β_1 sequence segments mediating the interaction with the α_1 subunit may also be involved in the homodimerization of β_1. Employing the yeast interaction trap assay we could demonstrate that β_1[1–348] embedding the entire N-terminal binding site readily interacts with β_1[349–403] holding major part of the C-terminal binding site and that both constructs tended to self-associate, whereas β_1[404–619] comprising the catalytic domain failed to interact (not shown). In line with these observations myc-tagged full-length β_1 coprecipitated with β_1[204–619] but not with the shorter forms of β_1[302–619] and β_1[379–619] from COS cell lysates (Fig. 6*A*). Also, the C-terminal deletion mutant of β_1[1–408] was recovered from precipitates of His_6-tagged full-length β_1 with Ni^{2+}-agarose (Fig. 6*B*). In COS cells cotransfected with His_6-tagged β_1 and EGFP-β_1[200–408] we detected the EGFP fusion protein applying Ni^{2+}-agarose (Fig. 6*C*). Finally, we were able to precipitate full-length β_1 from lysates of cells coexpressing β_1 and VSV-β_1[204–408] using anti-VSV (Fig. 7*A*). Of note, the protein level of wild-type β_1 was significantly reduced by the coexpression of β_1[204–408] but not of control protein IA2βcyt (Fig. 7*B*), confirming and extending our previous conclusion that β_1[204–408] may bind to heteronymous (α) or homonymous (β) interaction partners and target them for intracellular degradation. Together these data demonstrate that the 204–408 region mediating α_1/β_1 heterodimerization is also involved in β_1/β_1 homodimerization.

DISCUSSION

Protein-protein interactions are among the fundamental mechanisms that help to shape the architecture of the cytoskeleton, to build up intracellular signaling networks, and to mediate the export and import over cellular membranes (30). Recent advances in the analysis of the human proteome have highlighted the multiplicity of interactions among cellular proteins, and many novel interactions are currently being identified by pull-down assays/mass spectrometry and fluorescence resonance energy transfer (FRET) techniques (31). Among the most frequent forms of protein interactions are homo- and heterodimerizations, which often depend on post-translational modifications of the binding partners. Dimerization is frequently entailed by changes in the location of proteins, by modulation of their ligand affinity, and/or by alteration of their enzymatic capacity. One such example is provided by sGC, a heterodimeric heme-containing enzyme representing the major intracellular NO receptor of mammalian cells.

The molecular mechanisms underlying sGC activity regulation have been studied extensively. By contrast, the structural basis of sGC heterodimerization has remained poorly understood, even though it has been known for more than a decade that association of the nascent α and β subunits is a key event in the formation of active sGC. The failure of previous attempts to produce active sGC enzyme by mixing recombinantly expressed α and β subunits further underlines this point (16). In a first step toward a deeper understanding of the molecular mechanisms underlying sGC heterodimerization we have mapped precisely the interactions site of the β_1 subunit of mammalian sGC. Our study has revealed several unexpected findings: first, the sequence segment mediating dimerization of β_1 extends over 205 residues (positions 204–408; herein referred to as the dimerization region) and covers sequences of the regulatory domain as well as the entire central region, *i.e.* the dimerization region of β_1 is more extended than previously thought (28, 29) stretching over a larger segment than the corresponding homodimerization region in the pGC subunits (27). Second, the β_1 dimerization region is bipartite, *i.e.* it has a minor N-terminal binding site (herein dubbed NBS) located in the regulatory domain and a major C-terminal binding site (CBS) situated in the central region. The main evidence that the CBS represents the major binding site is that (i) internal deletion mutants lacking the CBS bind α_1 more weakly than mutants lacking NBS, and that (ii) C-terminal mutant β_1[1–379] retaining NBS shows no binding, whereas N-terminal mutant β_1[304–619] retaining CBS shows weak binding to α_1. Third, the "isolated" dimerization region of β_1[204–408] appears to bind to both α_1 and β_1 and target them for proteasomal degradation, possibly following dissociation of the $\alpha_1\beta_1$ dimer. Our preliminary experiments support this latter possibility: coexpression of increasing amounts of β_1[204–408] with wild-type α_1 and full-length β_1 or shortened β_1 variants in the presence of MG132 indicated that β_1[204–408] can displace β_1, β_1[62–619] or β_1[204–619], although with grossly varying efficacy (not shown).

Because specific binding sites are often well conserved among mammalian species, we compared the human, mouse,

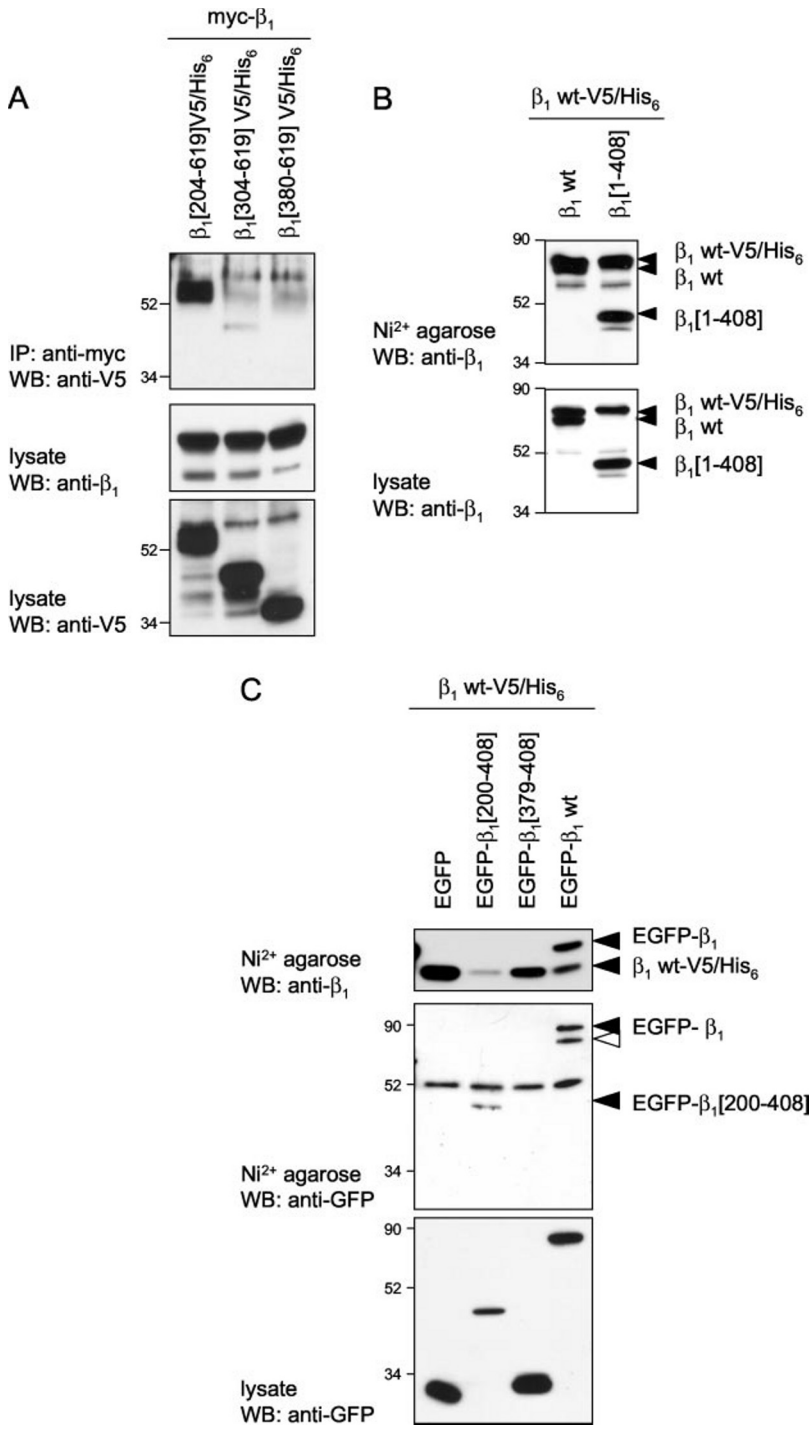

FIG. 6. **Mapping of segments involved in β_1 homodimer formation**. *A*, COS cells were cotransfected with cDNAs encoding myc-tagged full-length β_1 and V5-tagged β_1 mutants, as indicated. Immunoprecipitates (*IP*) with anti-myc were analyzed by Western blotting (*WB*) using anti-V5 (*top*). To monitor expression levels, lysates were blotted with anti-β_1 or anti-V5 (*middle* and *bottom*, respectively). *B*, COS cells were cotransfected with cDNAs encoding V5/His_6-tagged full-length β_1 and wild-type (*wt*) β_1 or β_1[1–408]. Ni^{2+}-agarose-bound His_6-tagged β_1 (*top*) or total cell lysates (*bottom*) were subjected to SDS-PAGE and blotted with anti-β_1. *C*, COS cells were cotransfected with cDNAs encoding V5/His_6-tagged β_1 and EGFP or EGFP fused to full-length β_1, β_1[200–408], or β_1[379–408]. Western blots of precipitates using Ni^{2+}-agarose were analyzed by anti-β_1 (*top*) or anti-GFP (*middle*). To monitor expression levels, lysates were blotted with anti-GFP (*bottom*). Blots are representatives of experiments repeated at least twice with identical results. The *open arrowhead* indicates proteolytic degradation product.

rat, and bovine sequences and found that the CBS sequences are identical among the various species and that only two conservative exchanges (Glu for Asp; Asp for Asn) occur in the corresponding NBS segments. Even for nonmammalian β subunits from *Drosophila melanogaster*, *Manduca sexta* and *Caenorhabditis elegans*, the sequence identity for the two predicted binding sites is well above their average sequence identity (41.5–96.7% *versus* 33–88%). Thus the two distinct binding sites have been well conserved through evolution, and one may anticipate that most, if not all, mammalian and nonmammalian sGCs use them. Given that we have characterized the dimerization region of β_1 in some detail, one may wonder about the corresponding site(s) in the α_1 subunit. Our preliminary mapping studies indicate that α_1 likely has a dimerization region extending over the regulatory domain and the central region and that the latter portion contains the major binding site, whereas the former appears to hold an accessory binding site.[2] Sequence comparisons of the relevant portions of α_1 and β_1 revealed an NBS-like sequence at positions 271–312 and a CBS-like sequence at positions 438–467 of rat α_1 with sequence identities of 46.3 and 50.0%, respectively, whereas the overall sequence identity among the two subunits is 29.8% (Fig. 8). Thus it is likely that the α_1 subunit holds a similar discontinuous binding module. Because β_1 may also interact with the α_2 subunit we compared the corresponding segments and found that the sequences of NBS (identity 43.9%; positions 312–352 of α_2) and CBS (56.7%; 477–506) are also well conserved among

[2] Z. Zhou, S. Gross, C. Roussos, S. Meurer, W. Müller-Esterl, and A. Papapetropoulos, unpublished experiments.

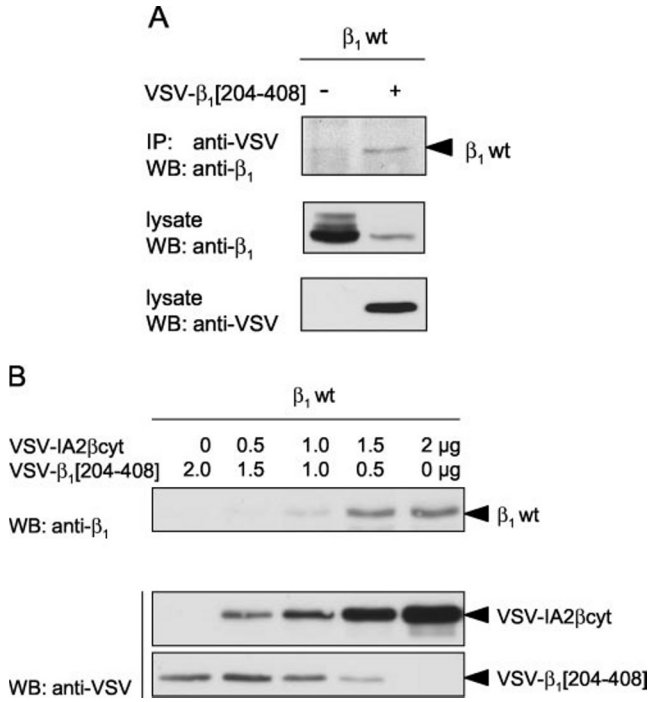

FIG. 7. **Expression of the dimerization region reduces β_1 levels.** *A*, COS cells were cotransfected with cDNAs encoding wild-type (*wt*) β_1 and VSV-tagged β_1[204–408]. Immunoprecipitates (*IP*) using anti-VSV were blotted with anti-β_1 (*top*). For control, lysates were blotted with anti-β_1 (*middle*) or anti-VSV (*bottom*). *WB*, Western blotting. *B*, COS cells expressing wild-type β_1 were cotransfected with varying amounts of cDNA encoding VSV-tagged β_1[204–408] (2.0–0 μg) or control protein IA2βcyt (0–2.0 μg). Protein levels were monitored by Western blotting of lysates using anti-β_1 (*top*) or anti-VSV (*bottom*). Blots are representative of experiments repeated at least twice with identical results.

NBS

α_1 ^{271}QSSLVIPTSLFCKTFPFHFMLDRDLAILQLGNGIRRLVNKRD^{312}
β_1 ^{204}QDS-RISPYTFCKAFPFHIIFDRNLVVTQCGNAIYRVLPQLQ^{244}
* * * *** **** ** * * ** * *

CBS

α_1 ^{438}AHQALEEEKKKTVDLLCSIFPSEVAQQLWQ^{467}
β_1 ^{379}TLRALEDEKKKTDTLLYSVLPPSVANELRH^{408}
*** ***** ** * * ** *

FIG. 8. **Sequence comparison of the NBS and CBS units in α_1 and β_1.** The homologous sequence segments of the rat α_1 (*upper line*) and β_1 subunit (*lower line*) are given for NBS (*top*) and CBS (*bottom*). Identical residues are marked by *asterisks*. Insertion of a single *gap* was allowed to optimize the alignment for NBS. *Numbers* indicate the relative positions in the amino acid sequence of the sGC subunits.

this subunit combination. Throughout the comparisons, the CBS sequence was less variant than the NBS sequence, and these data may reflect the dominance of CBS over NBS.

What are the relative orientations of the binding sites exposed by α_1 and β_1 subunits? At this time we cannot provide conclusive experimental evidence for a parallel or an antiparallel arrangement; however, the fact that both the regulatory and the catalytic domains of α_1 and β_1 show structural and functional complementation clearly favors the parallel model. It is conceivable that two sites are juxtaposed in the native conformation of sGC such that the CBS segment of one subunit may bind to both NBS and CBS of the other subunit, and vice versa. The parallel arrangement of the two subunits would also provide an intuitive answer to the question why heterodimerization of the sGC subunits is favored over homodimerization in native cells (22). Because three domains (regulatory, central, catalytic) complement each other in the heterodimer and only a single one (central) in the homodimer, one may predict that the former process is kinetically favored over the latter.

An unanticipated finding of this study is the identification of two distinct binding sites within a contiguous dimerization region of β_1 which appear to cooperate in α_1 binding. Perhaps the best evidence for this claim comes from the failing of the fused individual binding sites (positions 204–244 and 379–408) to confer α_1 binding competence to EGFP. Hence the intervening sequence (245–378) likely contributes to the formation of a functional binding region, probably by bringing NBS and CBS in proximity such that they can bind jointly to α_1. Our preliminary finding that a deletion mutant $\beta_1\Delta$304–379 lacking major part of the intervening sequence has reduced binding affinity for α_1[3] lends further credit to this notion. Another surprising finding is the dominant-negative role of the isolated dimerization region β_1[204–408] binding to the native subunits and targeting them for degradation, most likely via the proteasome. Binding of β_1[204–408] appears to have a greater impact on the stability of α_1, as indicated by our findings that α_1 protein was more readily down-regulated than β_1 protein and that β_1[204–408] was readily detected in β_1 but not in α_1 coimmunoprecipitates. These phenomena might relate to the fact that only β_1 but not α_1 interacts with and is stabilized by heat shock protein hsp90 (6). It is tempting to speculate that expression of alternatively spliced variants or isoforms of the β subunit exposing modified N- or C-terminal portions but retaining the dimerization region may contribute to the fine tuning of cellular cyclase activity through targeted degradation of the resultant complexes. Notably various isoforms of human and rat β_2 expressed in kidney, liver, and brain (19, 32) are characterized by N-terminal truncations of up to 79 residues and C-terminal extensions of up to 63 residues compared with the corresponding β_1 subunits (19, 33, 34). Among these, the rat β_2 isoform has been shown to reduce considerably the activity of coexpressed $\alpha_1\beta_1$ *in vitro*, and therefore enhanced expression of β_2 has been implicated in the down-regulation of renal guanylyl cyclase activity in Dahl salt-sensitive rats (35). Hence the mutual binding sites of sGC subunits may present interesting targets for therapeutic interventions aimed at modulating basal as well as NO-driven cGMP production in vascular cells.

Acknowledgments—We thank Dr. Carol Murphy for generously providing the 9E10 myc antibody and Dr. Katerina Kondili for help with the generation of the antiserum to α_1.

REFERENCES

1. Moncada, S., Palmer, R., and Higgs, E. (1991) *Pharmacol. Rev.* **43,** 109–142
2. Lucas, K. A., Pitari, G. M., Kazerounian, S., Ruiz-Stewart, I., Park, J., Schulz, S., Chepenik, K. P., and Waldman, S. A. (2000) *Pharmacol. Rev.* **52,** 375–414
3. Potter, L. R., and Hunter, T. (2001) *J. Biol. Chem.* **276,** 6057–6060
4. Humbert, P., Niroomand, F., Fischer, G., Mayer, B., Koesling, D., Hinsch, K. D., Gausepohl, H., Frank, R., Schultz, G., and Böhme, E. (1990) *Eur. J. Biochem.* **190,** 273–278
5. Hobbs, A. J. (1997) *Trends Pharmacol. Sci.* **18,** 484–491
6. Venema, R. C., Venema, V. J., Ju, H., Harris, M. B., Snead, C., Jilling, T., Dimitropoulou, C., Maragoudakis, M. E., and Catravas, J. D. (2003) *Am. J. Physiol.* **285,** H669–H678
7. Russwurm, M., Wittau, N., and Koesling, D. (2001) *J. Biol. Chem.* **276,** 44647–44652
8. Zabel, U., Kleinschnitz, C., Oh, P., Nedvetsky, P., Smolenski, A., Müller, H., Kronich, P., Kugler, P., Walter, U., Schnitzer, J. E., and Schmidt, H. H. (2002) *Nat. Cell Biol.* **4,** 307–311
9. Stone, J., and Marletta, M. (1994) *Biochemistry* **33,** 5636–5640
10. Brüne, B., Schmidt, K. U., and Ullrich, V. (1990) *Eur. J. Biochem.* **192,** 683–688

[3] Z. Zhou, S. Gross, C. Roussos, S. Meurer, W. Müller-Esterl, and A. Papapetropoulos, unpublished observation.

11. Friebe, A., Schultz, G., and Koesling, D. (1996) *EMBO J.* **15,** 6863–6868
12. Martin, E., Lee, Y. C., and Murad, F. (2001) *Proc. Natl. Acad. Sci. U. S. A.* **98,** 12938–12942
13. Stasch, J. P., Schmidt, P., Alonso-Alija, C., Apeler, H., Dembowsky, K., Haerter, M., Heil, M., Minuth, T., Perzborn, E., Pleiss, U., Schramm, M., Schroeder, W., Schroder, H., Stahl, E., Steinke, W., and Wunder, F. (2002) *Br. J. Pharmacol.* **136,** 773–783
14. Kamisaki, Y., Saheki, S., Nakane, M., Palmieri, J. A., Kuno, T., Chang, B. Y., Waldman, S. A., and Murad, F. (1986) *J. Biol. Chem.* **261,** 7236–7241
15. Buechler, W. A., Nakane, M., and Murad, F. (1991) *Biochem. Biophys. Res. Commun.* **174,** 351–357
16. Harteneck, C., Koesling, D., Soling, A., Schultz, G., and Böhme, E. (1990) *FEBS Lett.* **272,** 221–223
17. Harteneck, C., Wedel, B., Koesling, D., Malkewitz, J., Böhme, E., and Schultz, G. (1991) *FEBS Lett.* **292,** 217–222
18. Nakane, M., Arai, K., Saheki, S., Kuno, T., Buechler, W., and Murad, F. (1990) *J. Biol. Chem.* **265,** 16841–16845
19. Yuen, P. S., Potter, L. R., and Garbers, D. L. (1990) *Biochemistry* **29,** 10872–10878
20. Mergia, E., Russwurm, M., Zoidl, G., and Koesling, D. (2003) *Cell. Signal.* **15,** 189–195
21. Russwurm, M., Behrends, S., Harteneck, C., and Koesling, D. (1998) *Biochem. J.* **335,** 125–130
22. Zabel, U., Häusler, C., Weeger, M., and Schmidt, H. H. (1999) *J. Biol. Chem.* **274,** 18149–18152
23. Andreopoulos, S., and Papapetropoulos, A. (2000) *Gen. Pharmacol.* **34,** 147–157
24. Koesling, D., and Friebe, A. (1999) *Rev. Physiol. Biochem. Pharmacol.* **135,** 41–65
25. Wedel, B., Humbert, P., Harteneck, C., Foerster, J., Malkewitz, J., Böhme, E., Schultz, G., and Koesling, D. (1994) *Proc. Natl. Acad. Sci. U. S. A.* **91,** 2592–2596
26. Koglin, M., and Behrends, S. (2003) *J. Biol. Chem.* **278,** 12590–12597
27. Wilson, E. M., and Chinkers, M. (1995) *Biochemistry* **34,** 4696–4701
28. Nighorn, A., Byrnes, K. A., and Morton, D. B. (1999) *J. Biol. Chem.* **274,** 2525–2531
29. Zhao, Y., and Marletta, M. A. (1997) *Biochemistry* **36,** 15959–15964
30. Mayer, B. (1999) *Mol. Biotechnol.* **13,** 201–213
31. Figeys, D. (2002) *Curr. Opin. Mol. Ther.* **4,** 210–215
32. Okamoto, H. (2004) *Int. J. Biochem. Cell Biol.* **36,** 472–480
33. Koglin, M., Vehse, K., Budaeus, L., Scholz, H., and Behrends, S. (2001) *J. Biol. Chem.* **276,** 30737–30743
34. Behrends, S., and Vehse, K. (2000) *Biochem. Biophys. Res. Commun.* **271,** 64–69
35. Gupta, G., Azam, M., Yang, L., and Danziger, R. S. (1997) *J. Clin. Invest.* **100,** 1488–1492